Research Article GU J Sci 32(3): 853-869 (2019) DOI: 10.35378/gujs.375313

Gazi University

Journal of Science

http://dergipark.gov.tr/gujs

Comparative Analysis of P & O and RBFN MPPT Controller Based Three Level SEPIC Topology for 1.2kW Solar PV System

Damodhar REDDY[1], Sudha RAMASAMY[2]

[1]*Department of Electrical and Electronics Engineering, HITAM, Hyderabad, India*

[2]*Department of Production Systems, University West, Trollhattan, Sweden*

Highlights

- Design of 1.2kW solar PV system with "SUNPOWER-305-WHT" panel.
- Radial Basis Function Network algorithm for maximum power point tracking.
- A Three-Level SEPIC topology as DC-to-DC converter for enhanced output voltage.
- Performance analysis of P & O and RBFN MPPT control algorithms.
- Result analysis of a 3-Level SEPIC topology with P & O and RBFN algorithms.

Article Info

Received: 05/01/2018
Accepted: 12/11/2018

Keywords

Solar PV System
MPPT
P & O Control Method
RBFN Control Algorithm
3-level SEPIC Topology

Abstract

This paper accords an intelligent controller based 3-level SEPIC configuration for energy transformation in the solar PV system. An artificial intelligence based radial basis function network is engaged as a control algorithm for the maximum power extraction and the converter control can be done based on the duty cycle generated by the controller. In this system, a SEPIC topology is used for high voltage gain with reduced switching losses. In this paper, an RBFN controller based 3-level SEPIC topology is designed for 1.2kW solar PV system over the traditional P & O (Perturb & Observe) control method and the comparative result analysis is done though the simulation output for the corresponding input parameters.

1. INTRODUCTION

The solar photovoltaic based power supply modules are the most popular & wide range installed renewable energy systems [1] in the power sector, due to immense advancement in low cost and highly efficient PV Panel design, MPPT control techniques and power conversion units [2]. On the other hand, continues changes in the price of fossil fuels led to the installation of renewable energy based alternative systems which result in effective utilization of natural resources [3, 4]. In the literature, there are various MPPT control techniques are proposed [5-7] by the researchers to obtain the optimal power point, namely incremental conductance (INC), P & O method by hill climb search method, fuzzy logic [8, 9] and artificial intelligence based controllers [10, 11] etc. The perturbation & observation and hill climb methods are regularly used MPPT control algorithm in various energy conversion units [12] due to simple structures but limited by low power tracking capability and also have low accuracy [13, 14]. An ANN based MPPT control strategies, namely fuzzy logic, ANFIS (adaptive neuro-fuzzy inference system) and neural networks etc, are more accurate and fast convergent. Apart from all the control techniques, RBFN control technique is a fast and dynamic non-linear control method with minimum computational data. This is one of the feed forward controllers of the artificial neural network (ANN) [15, 16] with simple in design structure and fast in convergence. This kind of MPPT controllers are essential for solar power system to trace the maximum power point & also controls the converter operation based on duty cycle.

*Corresponding author, e-mail: ishuma@gmail.com

Two-level converters play a significant role in renewable integration of solar PV with other existing power systems to enhance the voltage levels with minimum operating losses. Due to low efficiency, low power density and high voltage stress across the switches [17-19], this kind of converters are replaced by the 3-level converters with high power density and reduced switching losses. The 3-level converters are widely [20-22] used in the solar PV systems for DC/DC conversion with enhanced voltage levels, low ripple current and minimized losses. In this paper RBFN controller based three level SEPIC configuration is designed for 1.2kW solar PV system. The design configuration is employed for variable irradiations.

2. SOLAR PV SYSTEM

The proposed solar power system configuration is as shown in Figure 1, in which the PV voltage (V_{PV}) & current (I_{PV}) are picked as input to the controller for optimal power point extraction at variable irradiations. The output of MPPT control algorithm is used to estimate the duty cycle and same is applied to the PWM controller where the pulses have to be generated for the converter switches. A 3-level SEPIC circuit topology is employed for boost function with reduced switching losses. The desired output voltage is obtained by estimating the proper duty cycle for optimal output voltage and power.

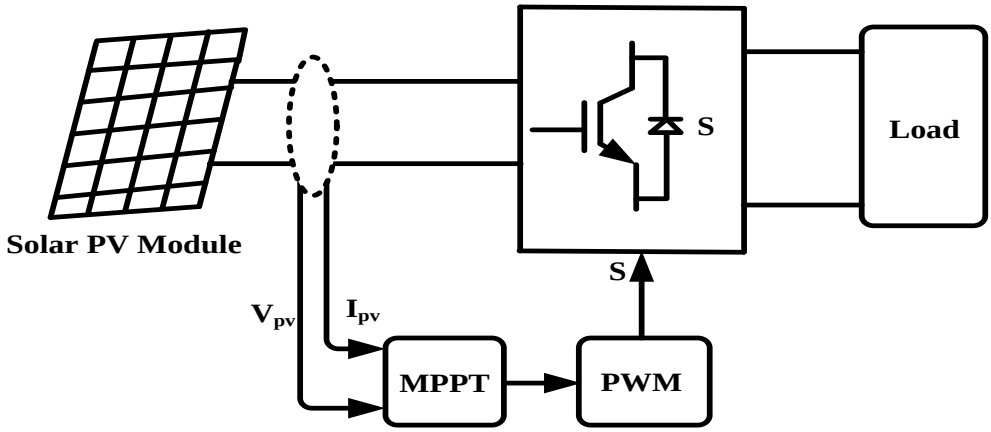

Figure 1. *Model representaion of proposed solar PV configuratioin*

2.1. Photovoltaic Cell

A simple and accurate single diode cell is designed to grab solar energy, in the form of temperature & irradiance and it is transformed into direct current. The photovoltaic cell designed in such a way that the desired voltage or current is to be achieved as the PV cells are formed in series or parallel configuration. The resultant circuit of PV cell is displayed in Figure 2 and the design parameters of current are derived from the Equations (1), (2) and (3). Similarly, the design parameters of PV array are also tabulated in Table 1.

$$I = I_{pv} - I_s(\exp\left[\frac{q(v+IR_s)}{N_s k T_a} - 1\right]) - \frac{(V+IR_s)}{R_p}\Big], \tag{1}$$

$$I_{pv} = (I_{n,pv} + K_1\Delta T)\frac{G}{G_n}, \tag{2}$$

$$I_s = \frac{(I_{sc,n} + K_1\Delta TI)}{\exp[\frac{(v_{oc} + K_v\Delta T)}{N_s k(T_a/q)} - 1]}, \tag{3}$$

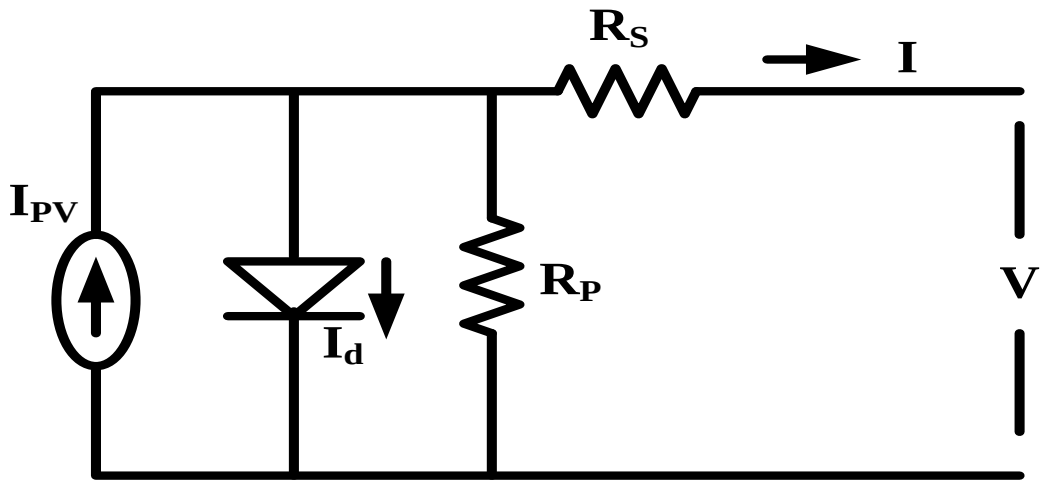

Figure 2. *Ideal circuit diagram of the solar PV cell*

where, I_{pv} = solar PV current, $I_{n,pv}$ = solar PV nominal current, q= Electron charge ($1.602x10^{-19}$ c), k= Boltzmann constant($1.38065x10^{-23}$J/K), a= Diode ideality constant, I_s= saturation current, I_{sc} = short circuit current, K_1= Ratio of short circuit current variation with temperature, K_v= Ratio of open circuit voltage variation with temperature, V_{oc} = open circuit voltage, N_s= number of arrays connected in series, T=Absolute temperature, ΔT= Deviation in temperature, T_n= Nominal temperature, G= Irradiance and G_n= Nominal irradiance.

In this proposed system, the SUNPOWER SPR-305-WHT-type array is chosen for 1.2kW solar PV system design with 2-series modules and 2-parallel strings as shown in the Figure 3.

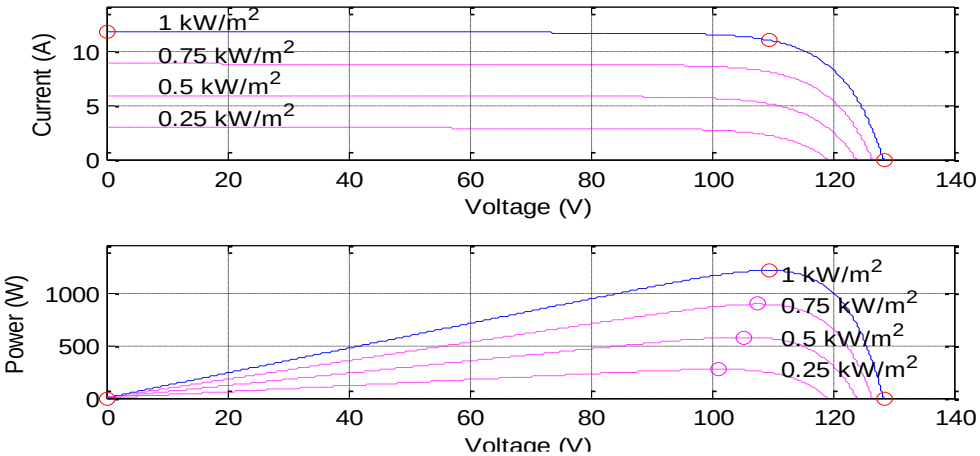

Figure 3. *P-V and I-V characteristics for SunPower-305-WHT PV array*

Table 1. *PV array parameters (SUNPOWER-305-WHT)*

S.No	Array parameters	Ratings
1	OC voltage (V_{oc})	64.2V
2	SC current (I_{sc})	5.96A
3	MPP voltage (V_{mp})	54.7V
4	MPP current (I_{mp})	5.58A
5	Series resistance (R_s)	0.03789Ω
6	Shunt resistance (R_p)	993.5 Ω
7	Diode current (I_{sat})	$1.17e^{-8}$A
8	Diode quality factor (Q_d)	1.3

2.2. Three Level SEPIC Topology

The 3-level SEPIC topology is shown in Figure 4, which employed as a DC to DC converter with the enhanced voltage level at the DC-link. The main role of SEPIC unit is to trnsform DC to DC with better conversion ratio [20-22]. For the boost operation of the converter, it has to be functioned at a duty cycle above 0.5. The circuit operation is elaborated in four modes by operating switches with proper switching pattern. The circuit parameters considered for aforementioned unit are tabulated in Table 2 for 1000W at 1000W/m^2 irradiation.

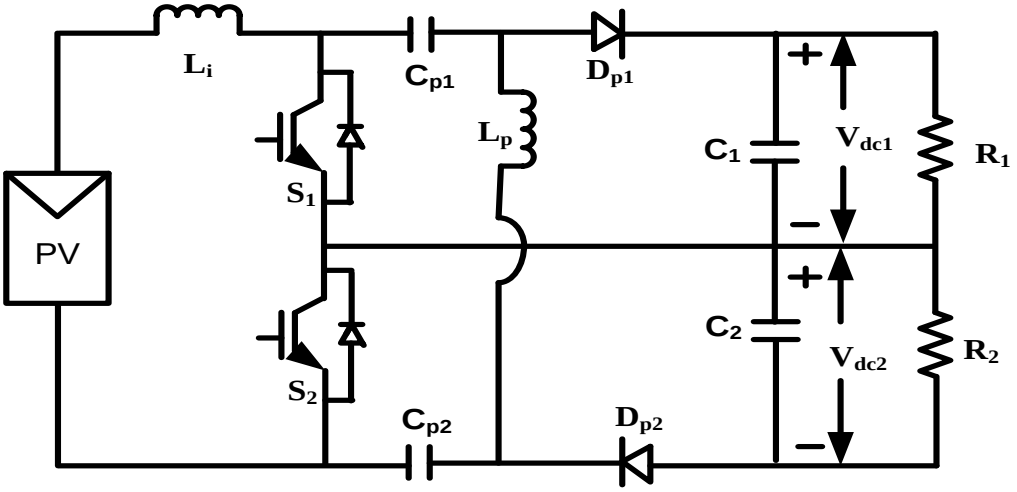

Figure 4. *Circuit diagram of 3-level DC/DC SEPIC converter*

Table 2. *Circuit parameters for 1000 W/m^2*

S.No	Circuit parameters	Ratings
1	Input voltage (V_{in}) from PV	110V
2	Maximum output voltage (V_{dc})	400V
3	Maximum output current (I_{dc})	2.5A
4	Maximum output power (P_{dc})	1.2kW
5	Input inductance (L_i)	4.5mH
6	Series capacitance (C_{p1}=C_{p2})	20μF
7	Parallel inductance (L_P)	4.5mH
8	Output capacitance (C_1+C_2)	200μF
9	Load resistance (R_1+R_2)	133.33Ω
10	Switching frequency (f_{sw})	20kHz

The circuit operation can be explained [20-22] in four modes as follows.

Mode 1: In this mode, switch S_1 and S_2 both are in ON state as shown in Figure 5, where the diode D_{p1} and D_{p2} are inactive. The source side inductor L_i start charging at the amount of $\frac{di_{Li}}{dt} = \frac{V_i}{L_i}$, through the switches S_1 and S_2 and the output inductor L_p charges the series capacitors C_{p1} and C_{p2} at the amount of $\frac{di_{Lp}}{dt} = \frac{V_i}{L_p}$, where the load side inductor current i_{Lp} pass through a path C_{p1}, S_1, S_2 and C_{p2}. Similarly, the output capacitors C_1 and C_2 discharge through the load R.

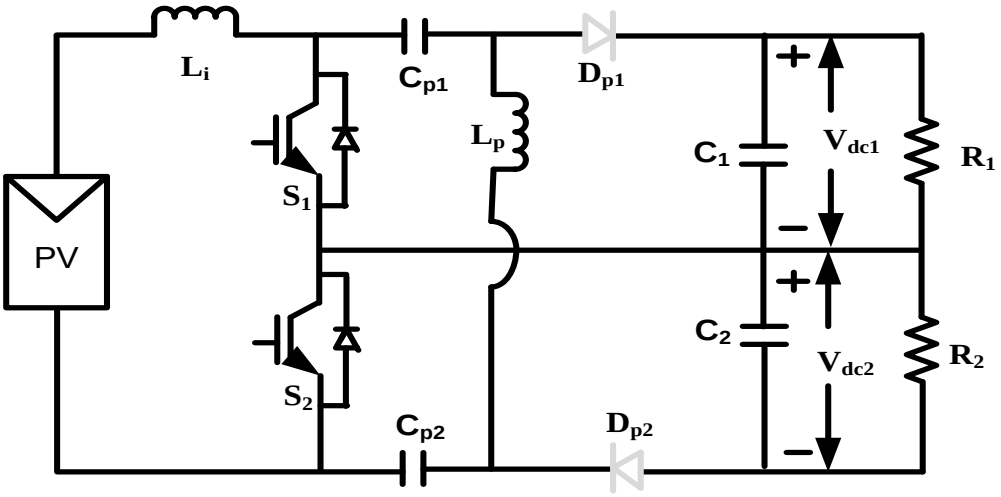

Figure 5. *Circuit diagram for switch S_1 and S_2 both are in ON state*

Mode 2: In this mode, switch S_1 is in ON state and S_2 is in OFF state as shown in Figure 6, where the diode D_{p1} is inactive and D_{p2} is active. The source side inductor L_i starts to charge through the series capacitor C_{p2} and output capacitor C_2, where the inductor current i_{Li} pass through a path L_i, S_1, C_2, D_{p2} and C_{p2} at the rate of $\frac{di_{Li}}{dt} = \frac{V_i - V_o}{2L_i}$. The load side inductor L_p charge via series capacitor C_{p1} and output capacitors C_2, where the output inductor current i_{Lp} flows through a path C_{p1}, S_1, C_2 and D_{p2} at the rate of $\frac{di_{Lp}}{dt} = \frac{V_i - V_o}{2L_p}$. Similarly the output capacitors C_1 and C_2 discharge through the load R.

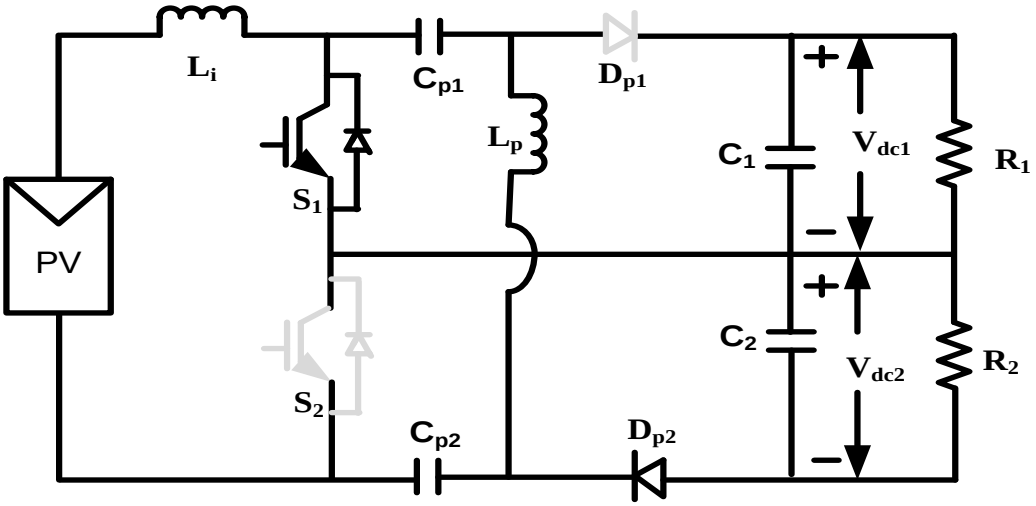

Figure 6. *Circuit diagram for switch S_1 is in ON and S_2 is in OFF state*

Mode 3: In this mode, switch S_2 is in ON state and S_1 is in OFF state as shown in Figure 7, where diode D_{p1} is active and D_{p2} is inactive. The source side inductor L_i charges through the capacitors C_{p1} and C_1, where the inductor current i_{Li} flows through a path L_i, C_{p1}, $D_{p1,}$ C_1 and S_2 at the amount of $\frac{di_{Li}}{dt} = \frac{V_i - V_o}{2L_i}$. The load side inductor L_p charges the series capacitor C_{p2} and output capacitor C_1 at the amount of $\frac{di_{Lp}}{dt} = \frac{V_i - V_o}{2L_p}$, where the inductor current i_{Lp} pass via D_{p1}, C_1, S_2, and C_{p2}. Similarly the output capacitors C_1 and C_2 discharge through the load R.

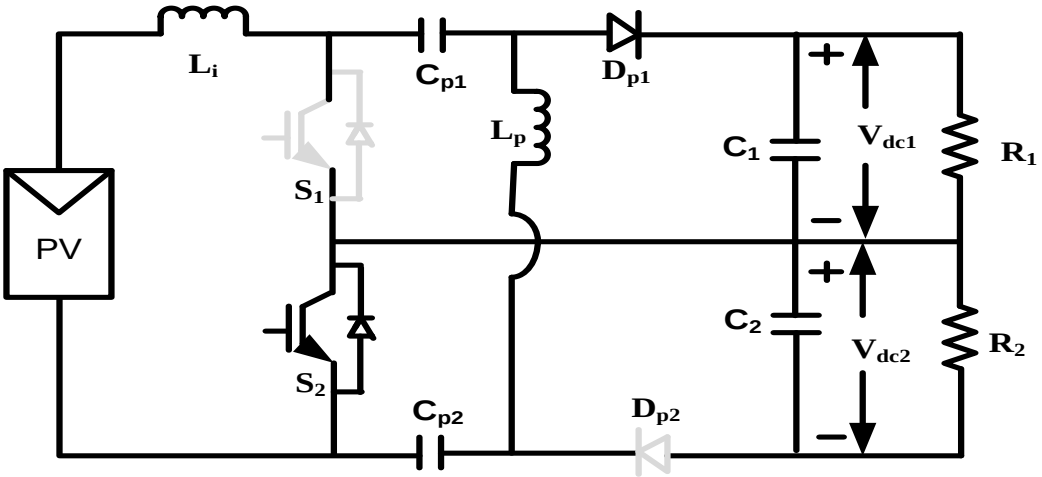

Figure 7. *Circuit diagram for switch S_1 is in OFF and S_2 is in ON state*

Mode 4: In this mode, switch S_1 and S_2 both are in OFF state as shown in Figure 8, where the diode D_{p1} and D_{p2} are active. The source side inductor L_i releases to the output capacitors C_1 and C_2, where the inductor current i_{Li} pass through a path L_i, C_{p1}, D_{p1}, C_1, C_2, D_{p2} and C_{p2} at the amount of $\frac{di_{Li}}{dt} = -\frac{V_i}{L_i}$, and at the same time the series capacitors C_{p1} and C_{p2} discharges through the load R. Similarly, the output inductor current i_{Lp} flows through the a path D_{p1}, C_1, C_2 and D_{p2} at the amount of $\frac{di_{Lp}}{dt} = -\frac{V_i}{L_p}$.

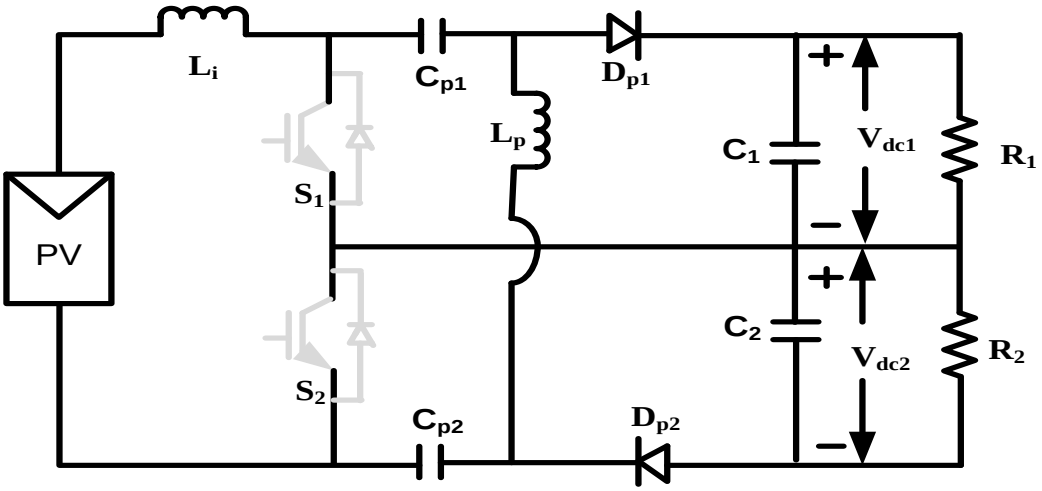

Figure 8. *Circuit diagram for switch S_1 and S_2 both are in OFF state*

From the Figure 4, the duty cycle D [20-22] can be written as $D = D_n + D_c$, where D_n is the nominal duty cycle and D_c is the control duty cycle.

$$D_n = \frac{V_o + V_{fD_p}}{V_o + V_{in} + V_{fD_p}}, \tag{4}$$

$$D_c = \frac{2L_i \Delta i_{Li}}{(V_o + V_{in} + V_{fD_p})T_s}, \tag{5}$$

where V_o= DC output voltage, $V_{in} = V_{PV}$ = Input voltage, V_{fD} = Diode forward voltage and T_s = Switching time. The input inductance of L_i can be written as

$$L_i = \frac{V_{in}.D_{\max}}{(\Delta i_L . f_{s(\min)})}, \tag{6}$$

where D_{max} =Maximum duty cycle, Δi_L = inductor ripple current, and f_s=switching frequency. And Δi_L can be written as,

$$\Delta i_L = 10\%.\frac{i_{in}}{\eta}$$, where η= Efficiency. (7)

The output capacitance C_o can be written as

$$C_o = \frac{i_o.D_{\max}}{(\Delta V_{Co} . f_{s(\min)})}, \tag{8}$$

where ΔV_C = capacitor ripple voltage, i_o = DC load current and DC-link capacitance = C_o= C_1 + C_2 .

$$\Delta V_{Co} = 10\%.\frac{V_{in}}{(1-D)}, \tag{9}$$

the output inductance of L_p can be written as

$$L_p = \frac{V_{in}.D_{\max}}{(\Delta i_L . f_{s(\min)})}, \tag{10}$$

the output capacitance C_p can be written as

$$C_p = \frac{i_{Li}.D_{\max}}{(\Delta V_{Cp} . f_{s(\min)})}, \tag{11}$$

where C_p = C_{p1} + C_{p2}, ΔV_{Cp} = Series capacitor ripple voltage and i_{Li} = Input current.

3. MPPT CONTROL METHODS

The proposed 3-level SEPIC configuration is analyzed and simulated for 1.2kW solar PV system. In this, the comparative analysis of the system is studied with P & O and RBFN based MPPT control algorithms for the same input parameters of the PV array and 3-level SEPIC configuration as shown in Tables 1 and 2 respectively.

3.1. Perturb & Observe Method

The perturb and observe is an repitative method for optimal power point extraction in solar PV systems. In this method, the maximum power point (MPP) extraction depends on estimation of the voltage and current of PV module. The module power is found to compared with the prior value [2, 6] which will give error in power value. The voltage is changes as the difference in power at module power increased $(\frac{dP_{PV}}{V_{PV}} > 0)$.

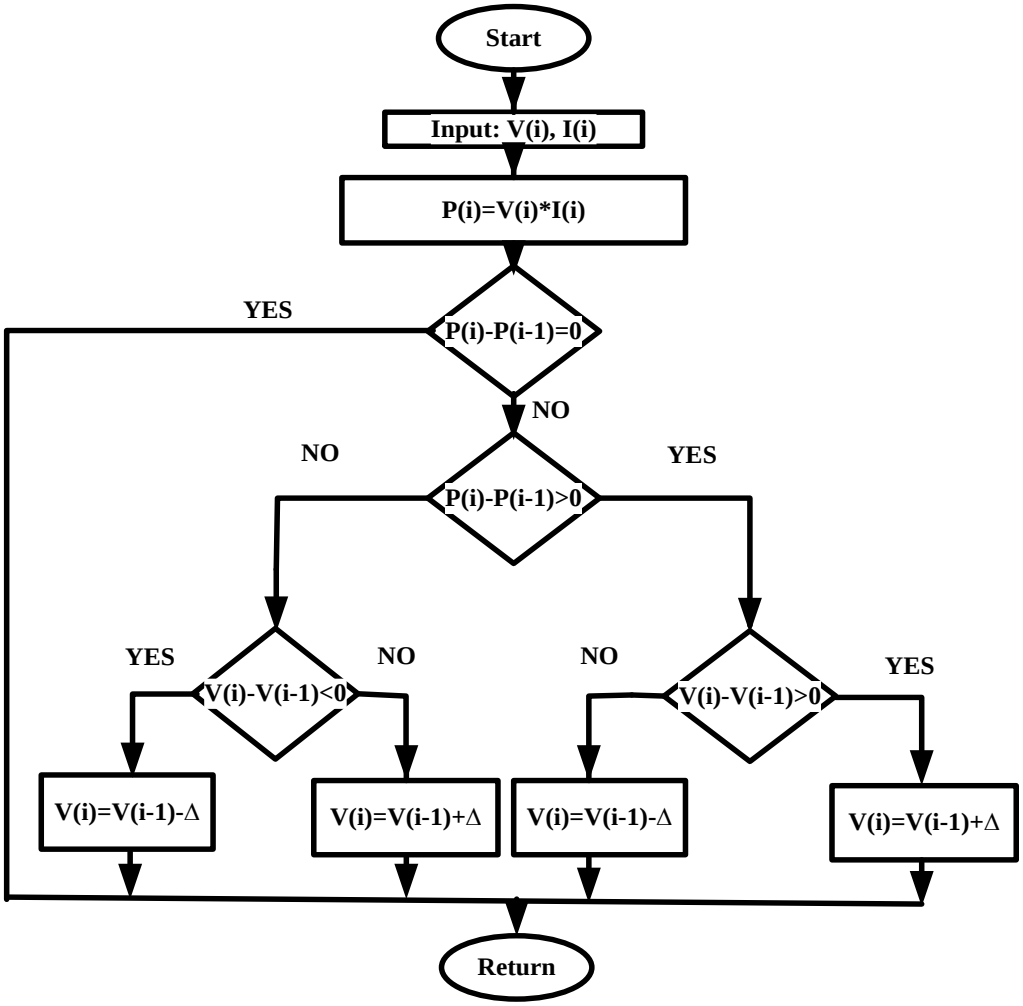

Figure 9. *Flowchart for P & O MPPT method*

The output voltage of the converter is depends on the duty cycle, where the P & O MPPT works on optimal power point extraction; the power tracking speed of the system is depends on the perturbation of the voltage. Perturb & Observe is a simple in structure and it does not require a prior knowledge on PV characteristics. If the perturbation is low then the response of the system to meet MPP is low, and as perturb is high then the response of the system is high. Figure 9 represents the flowchart of P & O MPPT control method.

3.2. RBFN Control Method

In the present scenario, artificial intelligent techniques are more popular over the traditional control techniques due to the fast and dynamic response of the system with non-linear system control capability. Artificial Neural network based RBFN controller is easy to implement with very less computational input data even for wide variations in the input. The optimal power point tracking of proposed configuration can be obtained by considering the solar PV module output parameters, namely voltage and current as the input variables to the RBFN control algorithm. The input data is trained in such way that the converter is controlled to get the desired output voltage, where the output of the controller is a duty cycle. It consists of three layers such as input layer, a hidden layer, and an output layer. The activation functions of the hidden layer are determined by using the distance between input vector and prototype vector. The input variables (x_i^1) to an RBFN controller are voltage and current, and the output variable (y_k^3) is a duty cycle (D) [5, 6]. The controller output as shown in Figure 10 is fed to the PWM (Pulse Width Modulation) generator through which the switching pulses are generated for the converter. The input variables taken for RBFN control configuration are presented in Table 3.

a) Input layer:

The measured input variables are directly transmitted to the next level through the nodes. The net input and output is [5, 6] represented as

$$x_i^1(N) = net_i^1 \tag{12}$$

$$y_i^1(N) = f_i^1(net_i^1(N)) = net_i^1(N),$$

where, i=1, 2,...,n. (13)

b) Hidden layer:

A Gaussian function is performed for each and every node i.e. an RBFN is used as a membership function. The net input and output for the hidden layer is [5, 6] represented as

$$\text{net}_j^{\,2}(\text{N}) = (\text{X} - \text{M}_j)^{\text{T}} \sum_{\text{j}} (\text{X} - \text{M}_j) \tag{14}$$

$$y_j^{\,2}(N) = f_i^{\,2}(net_j^{\,2}(N)) = Exp(net_j^{\,2}(N)),$$

j=1, 2,…..,9, (15)

where Mean, $M_j = [m_{1j} m_{2j} \ldots\ldots m_{ij}]^T$ and

Standard deviation,

$$\sum_j = diag[\frac{1}{\sigma_{1j}^{\,2}} \frac{1}{\sigma_{2j}^{\,2}} \ldots\ldots\ldots \frac{1}{\sigma_{ij}^{\,2}}]^T.$$

c) Output layer:

The overall output can be computed by the summation of all the inputs through the single node k, which is represented as $\sum$, therefore

$$net_k^{\,3} = \sum W_j y_j^{\,2}(N) \tag{16}$$

$$y_k^{\,3}(N) = f_k^{\,3}(net_k^{\,3}(N)) = net_k^{\,3}(N) = D \tag{17}$$

The desired control mechanism is achieved by selecting the minimum of 617 input data from solar PV module and the the RBFN control algorithm has tuned to maintain the optimal operating point according to the change in the input parameters.

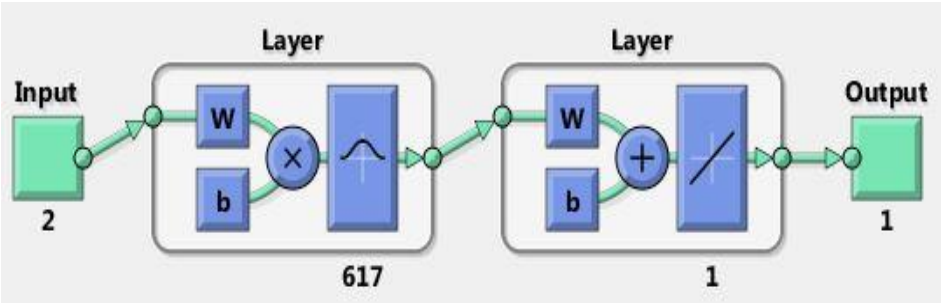

Figure 10. *RBFN Structure*

Table 3. *RBFN Control Parameters*

S.No	Control parameters	Values
1	Input variables	V_{PV} and I_{PV}
2	Output variables	D (Duty cycle)
3	Input Data (number of data values)	617
4	Training algorithm	OLS (Ordinary Least Squares) method
5	Speed factor	0.03

4. SIMULATION AND RESULT DISCUSSION

4.1. Perturb & Observe MPPT controller based solar PV system

In this system, a Perturb & Observe MPPT controller based 1.2kW three level SEPIC circuits for DC/DC conversion is designed for solar PV system at constant irradiation of 1000 W/m^2. The design variables considered for the proposed control configuration are tabulated in Table 2. The step-wise input irradiation is considered as input to solar PV array as shown in Figure 11.

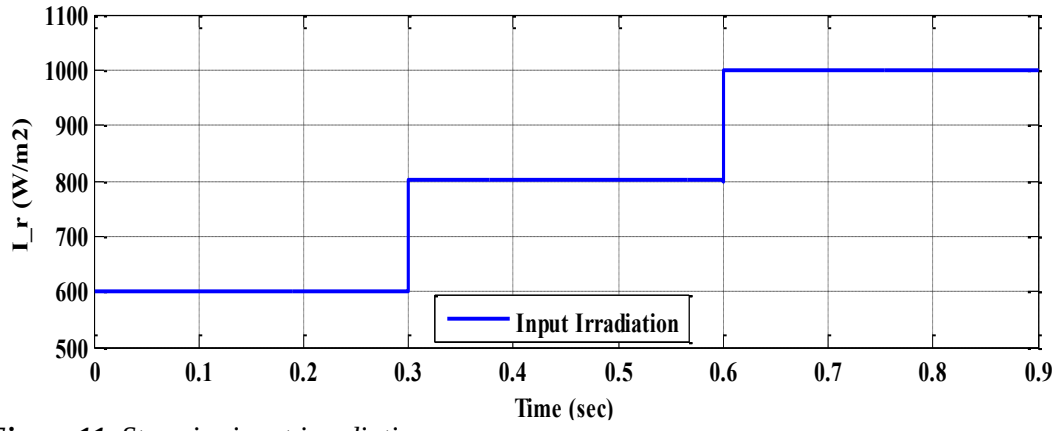

Figure 11. *Stepwise input irradiation*

The output of the PV array (voltage and current) is tabulated in Table 4 for corresponding irradiations at different time intervals as shown in Figure 12. The DC Output parameters of 3-level SEPIC are presented in Figure 13, namely voltage and current for various irradiations. The voltage across the DC-link capacitors of 3-level SEPIC is obtained in the desiged system as depicted in Figure 14, which results in the balanced system configuration for stable operation.

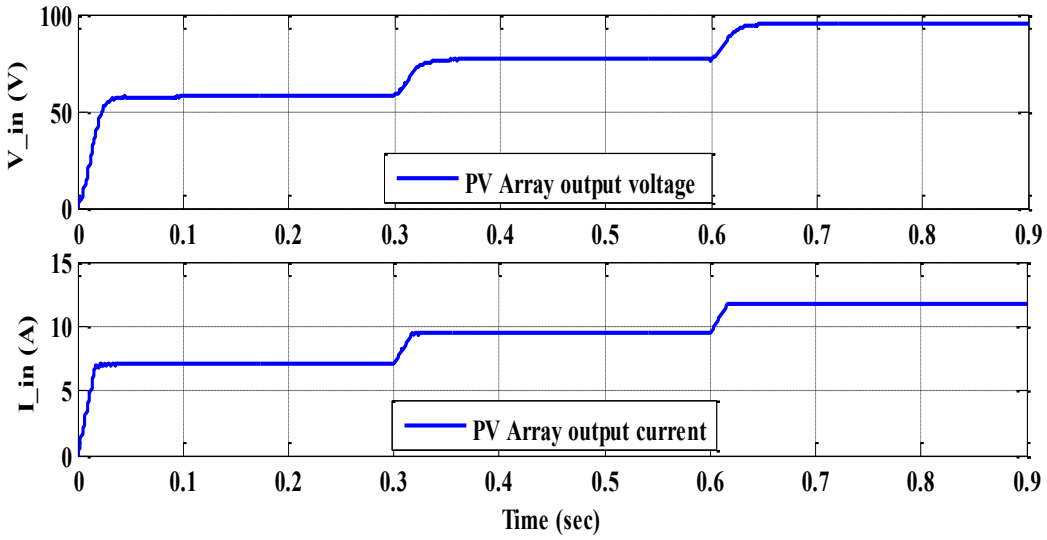

Figure 12. *Output voltage and current of PV Array using P & O*

Table 4. *PV array output parameters*

Time (Sec)	**0 to 0.3**	**0.3 to 0.6**	**0.6 to 0.9**
Irradiation (W/m^2)	600	800	1000
PV voltage (V_{pv})	57.5V	76.6V	95.1V
PV current (I_{pv})	7.89A	9.46A	11.75A
PV power (P_{pv})	453.67W	724.64W	1107.42W

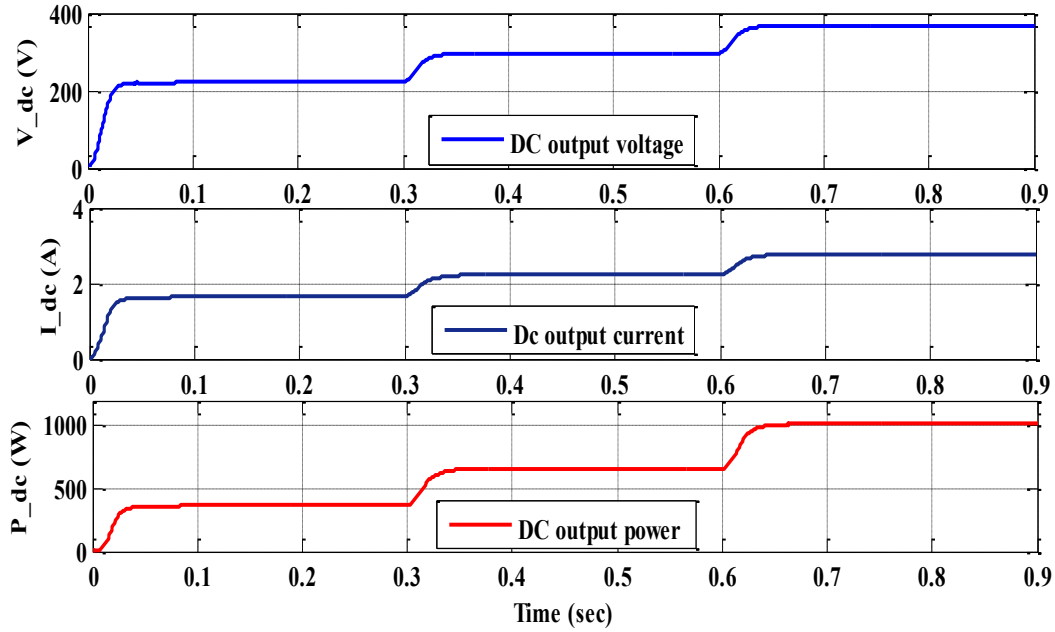

Figure 13. *DC Output voltage, current, and power of 3-level SEPIC*

The output voltage of 3-level SEPIC is obtained as 367.4V, the output current is obtained 2.75A and the output power of 3-level SEPIC is 1012W. The DC link capacitor voltages of 183.7V and 183.7V are equally distributed across the capacitors $C_1$and. The complete result analysis of the 3-level SEPIC is tabulated in Table 5 for different time intervals and irradiations.

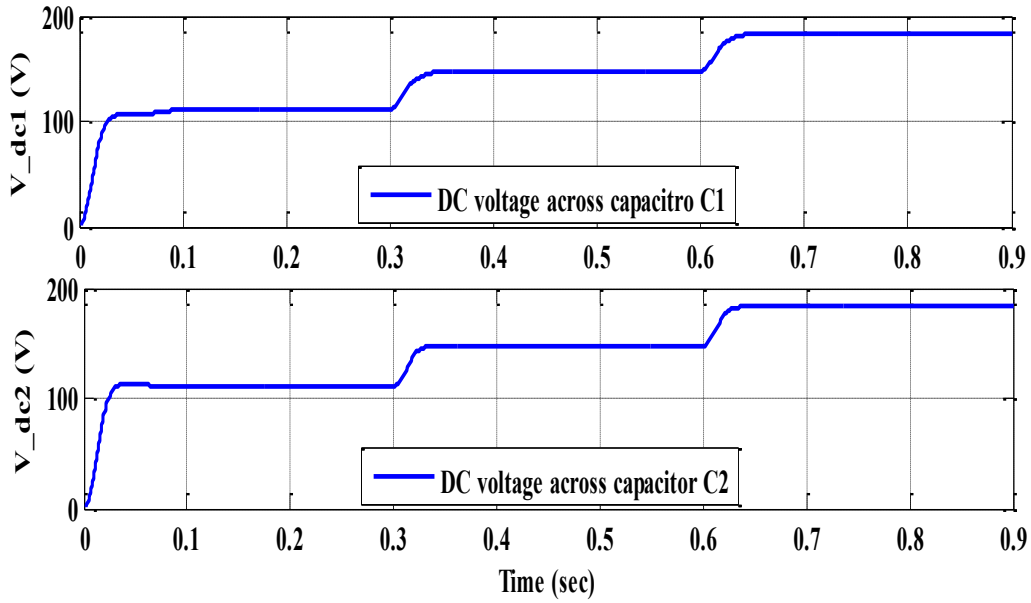

Figure 14. *DC-link voltage of 3-level SEPIC converter*

Table 5. *Output Parameters of the 3-level SEPIC with P & O MPPT control Algorithm*

Time (Sec)	**0 to 0.3**	**0.3 to 0.6**	**0.6 to 0.9**
Irradiation (W/m^2)	600	800	1000
Voltage (V_{dc})	221.7V	295.5V	367.4V
Current (I_{dc})	1.66A	2.217A	2.75A
Power (P_{dc})	368.5W	655.3W	1012W
Capacitor C_1 voltage (V_{c1})	110.8V	147.9V	183.7V
Capacitor C_2 voltage (V_{c2})	110.8V	147.9V	183.7V

4.2. RBFN MPPT controller based solar PV system

In this system, an RBFN MPPT controller based 1.2kW three level SEPIC circuit for DC/DC conversion is designed for solar PV system at 1000 W/m^2 irradiation. The output of the PV array (voltage and current) is tabulated in Table 6 for corresponding irradiations at different time intervals as depicted in Figure 15. The DC Output parameters of 3-level SEPIC are represented in Figure 16, namely voltage, current and power for various irradiations. The equal distribution of voltage across the DC-link capacitors of 3-level SEPIC is obtained in the designed system as depicted in Figure 17, which results in the balanced system configuration for stable operation.

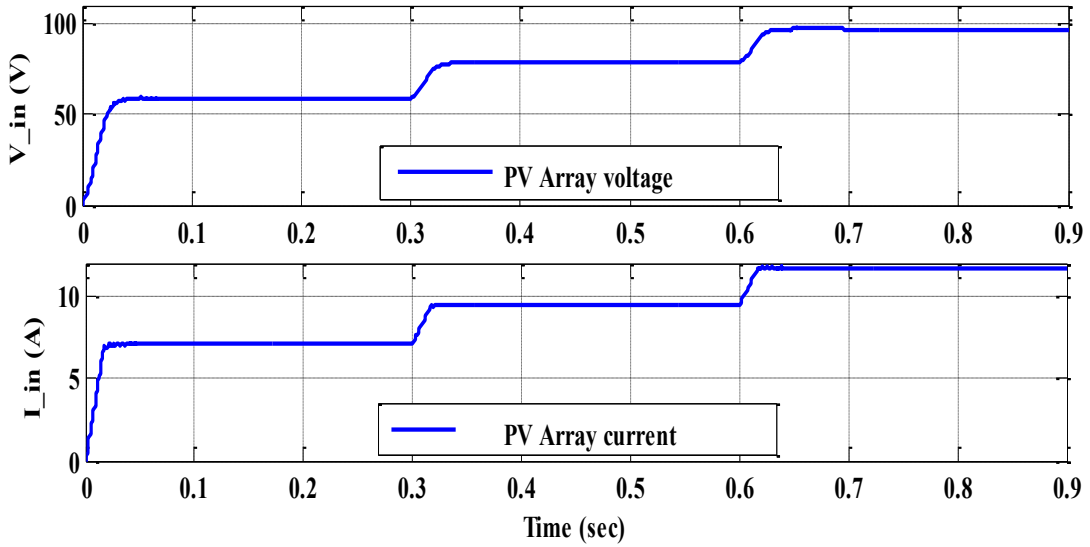

Figure 15. *PV Array output voltage and current using RBFN*

Table 6. *PV array output parameters*

Time (Sec)	**0 to 0.3**	**0.3 to 0.6**	**0.6 to 0.9**
Irradiation (W/m^2)	600	800	1000
PV voltage (V_{pv})	58.8V	78.3V	96.9V
PV current (I_{pv})	7.09A	9.46A	11.73A
PV power (P_{pv})	460.4	740.7W	1126.6W

The output voltage of 3-level SEPIC is obtained as 374.5V, the output current is obtained 2.8A and the output power of 3-level SEPIC is 1052W. The DC link capacitor voltages of 187.3V and 187.3V are equally distributed across the capacitors C_1 and C_2. The performance analysis of the 3-level SEPIC is tabulated in Table 7 for different time intervals and irradiations.

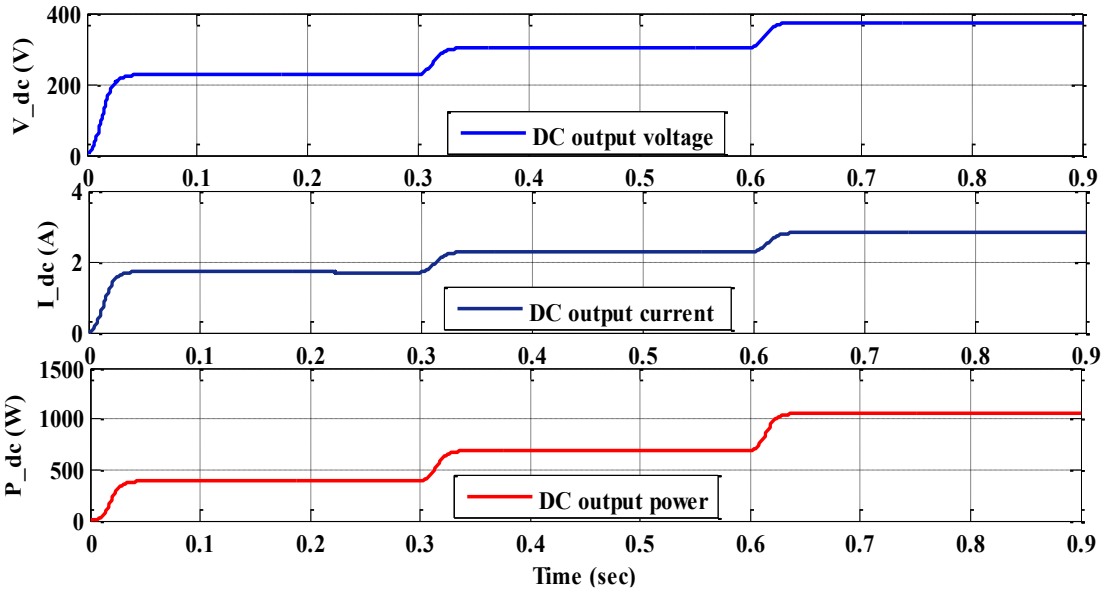

Figure 16. *DC Output voltage, current, and power of 3-level SEPIC*

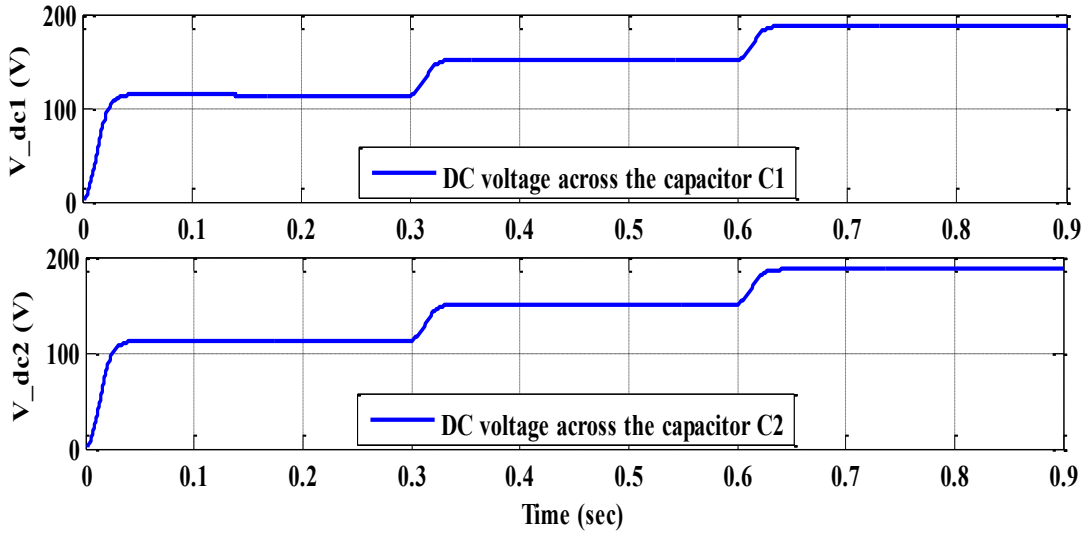

Figure 17. *The output capacitor voltages of the 3-level SEPIC converter*

Table 7. *Output Parameters of the 3-level SEPIC with RBFN MPPT algorithm*

Time (Sec)	**0 to 0.3**	**0.3 to 0.6**	**0.6 to 0.9**
Irradiation (W/m^2)	600	800	1000
Voltage (V_{dc})	226.5V	302.2V	374.5V
Current (I_{dc})	1.7A	2.26A	2.8A
Power (P_{dc})	386.6W	683.4W	1052W
Capacitor C_1 voltage (V_{c1})	113.4V	151.1V	187.3V
Capacitor C_2 voltage (V_{c2})	113.4V	151.1V	187.3V

The solar PV array power output is depicted in Figure 18 for different irradiations. Here, the power output of the solar PV array is plotted for both P & O and RBFN control algorithms and hence the result of the RBFN control is better than the Perturb & Observe method, in order to trace the accurate maximum power point.

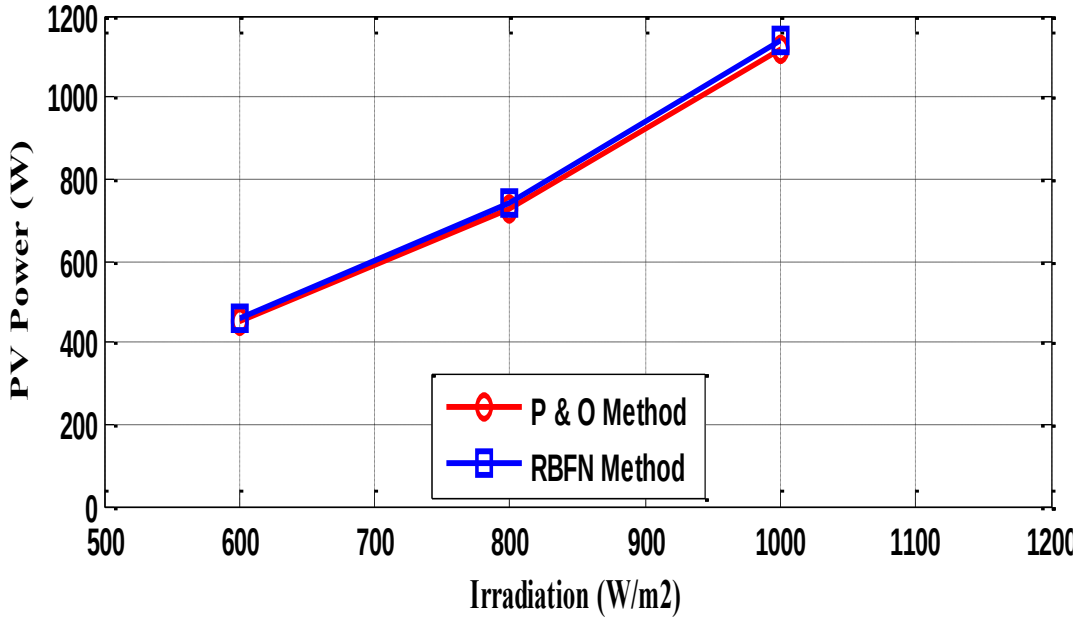

Figure 18. *PV output power at different irradiations*

The Figure 19 states that the converter efficiency with respect to the output power for different PV power output using both Perturb & Observe and RBFN MPPT control methods. Hence, the RBFN MPPT controller based converter circuit has a better efficiency of 93.37% than the P & O MPPT controller based converter circuit of 90.58% at a maximum power output of solar PV system.

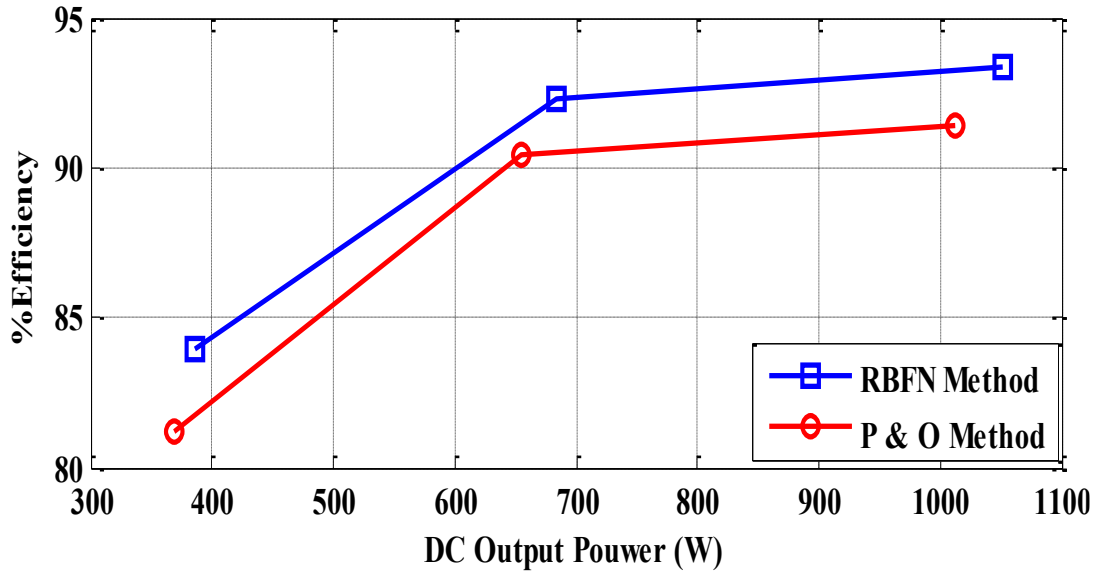

Figure 19. *Converter DC output power v/s %efficiency*

5. CONCLUSION

The design of 1.2kW SEPIC configuration is carried out for solar power system by using P & O and RBFN MPPT control algorithms. A comparative result analysis is carried out through MATLAB/Simulink at variable irradiations and at constant temperature. It is observed that the RBFN MPPT controller based converter circuit has shown a better efficiency of 93.37% than the P & O MPPT controller based converter circuit of 90.58% at a maximum power output of solar PV system. The 3-level SEPIC topology is having minimized voltage stress across the switches and switching losses. This kind of converter topologies is widely used in DC-to-DC conversion to enhance the voltage to the required level based on application. The boost type converter is essential in low power generating systems such as solar PV systems, fuel cells, and other DC supplied systems. The design configuration of MPPT control based 3-level SEPIC is an adequate system for solar PV systems with an improved efficiency.

CONFLICTS OF INTEREST

No conflict of interest was declared by the authors.

REFERENCES

[1] Joshi, K.A., Pindoriya, N.M., "Impact investigation of rooftop Solar PV system: A case study in India", 3rd IEEE PES Innovative Smart Grid Technologies Europe (ISGT Europe), 1-8, (2012).

[2] Kumar, K., Babu, N.R., Prabhu, K.R., "Design and analysis of RBFN-based single MPPT controller for hybrid solar and wind energy system", IEEE Access, 5:15308-17, (2017).

[3] Singh, B., Jain, C., Goel, S., Gogia, R., "Subramaniam U. A sustainable solar photovoltaic energy system interfaced with grid-Tied Voltage source converter for power quality improvement", Electric Power Components and Systems, 45(2):171-83, (2017).

[4] Jain, C., Singh, B., "A three-phase grid tied SPV system with adaptive DC link voltage for CPI voltage variations", IEEE Transactions on Sustainable Energy, 7(1):337-44, (2015).

[5] Messalti, S., Harrag, A., Loukriz, A., "A new variable step size neural networks MPPT controller: Review, simulation and hardware implementation", Renewable and Sustainable Energy Reviews, 68:221-33, (2017).

[6] Saravanan, S., Babu, N.R., "RBFN based MPPT algorithm for PV system with high step up converter", Energy Conversion and Management, 122: 239-51, (2016).

[7] Xiao, W., Edwin, F.F., "Spagnuolo G, Jatskevich J. Efficient approaches for modeling and simulating photovoltaic power systems", IEEE Journal of Photovoltaics, 3(1):500-8, (2012).

[8] El Khateb, A., Rahim, N.A., Selvaraj, J., Uddin, M.N., "Fuzzy-logic-controller-based SEPIC converter for maximum power point tracking", IEEE Transactions on Industry Applications, 50(4): 2349-58, (2014).

[9] Reddy, D., Ramasamy, S., "A fuzzy logic MPPT controller based three phase grid-tied solar PV system with improved CPI voltage", Innovations in Power and Advanced Computing Technologies (i-PACT), IEEE, 1-6, (2017).

[10] Singh, B., Shahani, D.T., Verma AK., "Neural network controlled grid interfaced solar photovoltaic power generation", IET Power Electronics, 7(3): 614-26, (2013).

[11] Reddy, D., Ramasamy, S., "Design of RBFN controller based boost type vienna rectifier for grid-tied wind energy conversion system", IEEE Access, 6: 3167-75, (2018).

[12] Ramasamy, S., Reddy, D., "Design of a three-phase boost type Vienna rectifier for 1kW wind energy conversion system", International Journal of Renewable Energy Research (IJRER), 7(4): 1909-18, (2017).

[13] Lyden, S., Haque, M.E., "A simulated annealing global maximum power point tracking approach for PV modules under partial shading conditions", IEEE Transactions on Power Electronics, 31(6) :4171-81, (2015).

[14] Gil-Antonio, L., Saldivar-Marquez, M.B., Portillo-Rodriguez, O., "Maximum power point tracking techniques in photovoltaic systems: A brief review", 13th International Conference on Power Electronics (CIEP), IEEE, 317-322, (2016).

[15] Lin, W.M., Hong, C.M., Ou, T.C., Chiu, T.M., "Hybrid intelligent control of PMSG wind generation system using pitch angle control with RBFN", Energy Conversion and Management, 52(2):1244-51, (2011).

[16] Ramasamy, S., "Single stage energy conversion through an rbfn controller based boost type Vienna rectifier in the wind turbine system", Gazi University Journal of Science 30(4): 253-66, (2017).

[17] Gules, R., Dos Santos, W.M., Dos Reis, F.A., Romaneli, E.F., Badin, A.A., "A modified SEPIC converter with high static gain for renewable applications", IEEE Transactions on Power Electronics, 29(11):5860-71, (2013).

[18] Chen, Y.M., Huang, A.Q., Yu, X., "A high step-up three-port DC–DC converter for stand-alone PV/battery power systems", IEEE Transactions on Power Electronics, 28(11):5049-62, (2013).

[19] Debnath, D., Chatterjee, K., "Two-stage solar photovoltaic-based stand-alone scheme having battery as energy storage element for rural deployment", IEEE Transactions on Industrial Electronics, 62(7):4148-57, (2014).

[20] Choi, W.Y., Lee, S.J., "3-level SEPIC with improved efficiency and balanced capacitor voltages", Journal of Power Electronics, 16(2):447-54, (2016).

[21] Choi, W.Y., "3-level single-ended primary-inductor converter for photovoltaic power conditioning systems", Solar Energy, 125:43-50, (2016).

[22] Yang, M.K., Lee, S.J., Heo, J., Choi, W.Y., "High-efficiency 3-level SEPIC for grid-tied PV systems", IEEE Energy Conversion Congress and Exposition (ECCE), 1-5, (2016).